Title

Assembly of the Tricyclic Core of Alopecurone C by Asymmetric Donor/Donor Carbene C—H Insertion

Journal

Organic Letters, 26(51)

ISSN

1523-7060

Authors

Shiue, Yuan-Shin

Dyer, Matthew W

Burlow, Noah P

et al.

Publication Date

2024-12-27

DOI

10.1021/acs.orglett.4c03863

Peer reviewed

OL Organic Letters

pubs.acs.org/OrgLett

Letter

Assembly of the Tricyclic Core of Alopecurone C by Asymmetric Donor/Donor Carbene C−H Insertion

Yuan-Shin Shiue, Matthew W. Dyer, Noah P. Burlow, Nutthakarn Soisaeng, Kellan N. Lamb, Cristian Soldi, James C. Fettinger, Dean J. Tantillo, and Jared T. Shaw*

Cite This: *Org. Lett.* 2024, 26, 11129−11133

Read Online

ACCESS | Metrics & More | Article Recommendations | Supporting Information

ABSTRACT: Two routes to assemble the complete tricyclic core of alopecurone C are described. In the first-generation route, an efficient synthesis of the "eastern" half of the target, including a decagram-scale rhodium-catalyzed C−H insertion reaction, was developed. When this route proved intractable for assembling the final flavanone ring, a successful second-generation route was developed from a flavanone precursor (naringenin) employing a later stage C−H insertion. Although the second route was ultimately unsuccessful for preparation of the final target, it does provide the basis for the efficient assembly of the complete tricyclic core of alopecurone C and related flavonostilbenoid natural products.

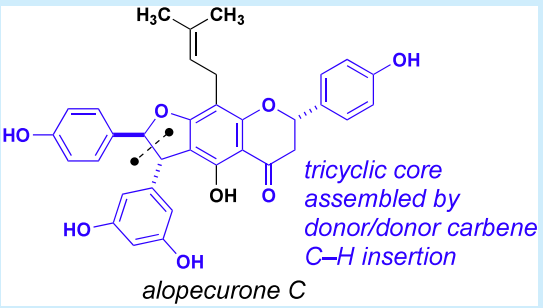

Plants biosynthesize a vast array of secondary metabolites for communication, defense, and other important survival functions. The shikimic acid pathway, which yields the aromatic amino acids, produces the phenolic compounds resveratrol (**1**) and naringenin (**2**) (Figure 1). Each of these

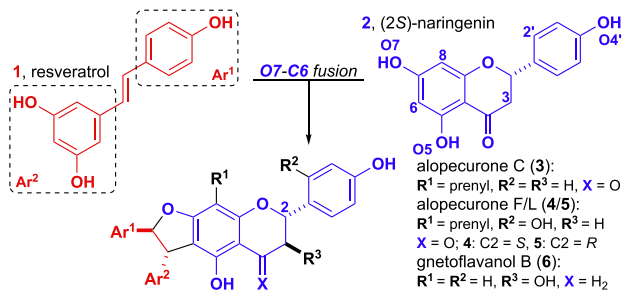

Figure 1. Biosynthetic origins and selected O7−C6 fused flavonostilbenoid natural products.

natural products have been implicated in a variety of biological effects in humans, given their occurrence in many foods and medicinal plants.[1,2] Moreover, resveratrol is known to form many complex natural products through dimerization and oligomerization that have subsequently been examined for biological activity and elegant syntheses.[3] Naringenin is also the progenitor of a wide range of complex natural products through subsequent oxidation, alkylation, glycosylation, oligomerization, etc.[4] Flavonostilbenes represent a point of convergence where these two common substructures are merged (Figure 1). The alopecurone family and related natural products emerge from regioselective ring formation between the double bond of resveratrol and the O7/C6 positions of naringenin. Two other possible modes of cyclization, i.e. C6/O5 and C8/O7, result in a series of related secondary metabolites.[4] To date, there are no reported syntheses of any flavonostilbene natural products.

The alopecurones are isolated from the roots of *Sophora alopecuroides*, which is a plant native to northern China and Mongolia.[5−7] Several studies have revealed cellular and organismal effects of these and related flavonostilbenes.[4,5,8] One study describes alopecurone C as having potent antimicrobial activity, i.e. minimum inhibitory concentrations (MICs) that are comparable to current antibiotics (<5 μg/mL) against more than 20 strains of methicillin-resistant *Staphylococcus aureus* (MRSA).[6] Dwindling natural stocks of *S. alopecuroides* have resulted in bans on harvesting root material,[7] which limits the extent to which these compounds can be evaluated further through isolation. As such, we have initiated a program to synthesize alopecurone C in order to generate larger supplies of the parent natural product and enable the preparation of analogs for structure−activity relationship (SAR) studies.

The key synthetic challenge to the synthesis of alopecurone C and related natural products is the densely substituted benzodihydrofuran core. Our group has established the asymmetric C−H insertion of donor/donor carbenes,[9−11] i.e. those substituted with two aromatic rings, as a highly efficient,

Received: October 28, 2024
Revised: December 4, 2024
Accepted: December 6, 2024
Published: December 12, 2024

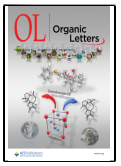

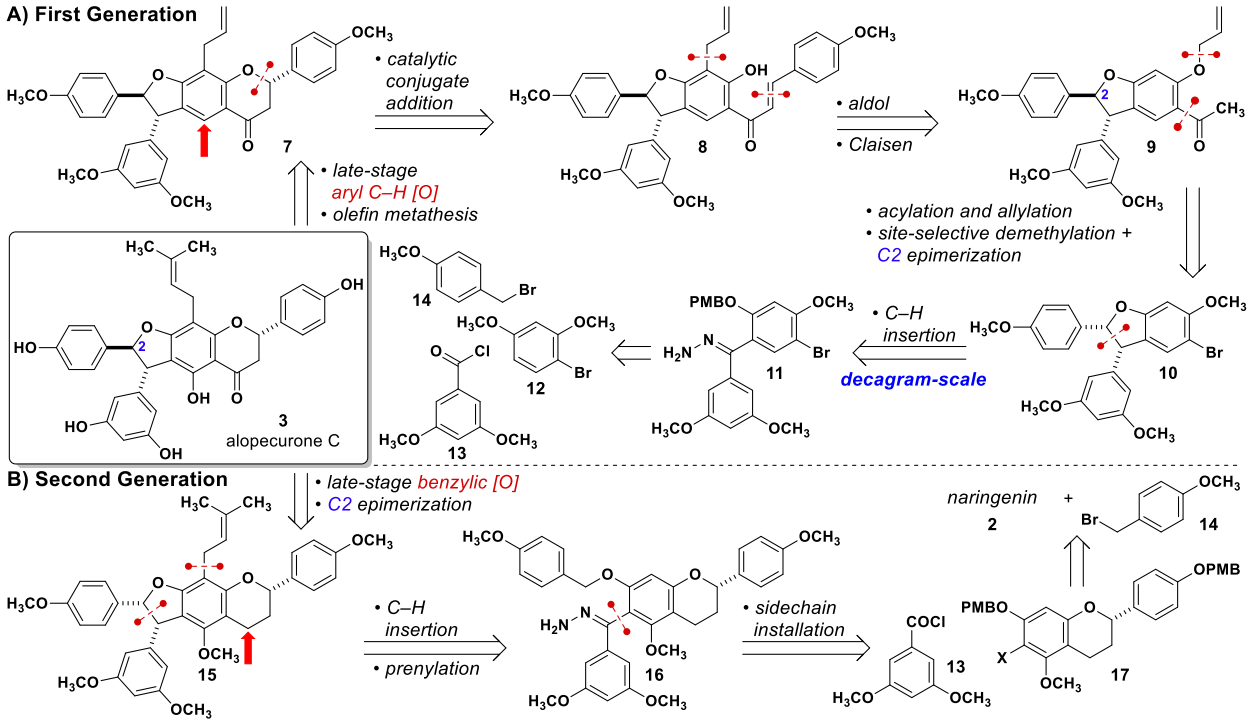

Figure 2. A) 1st Gen route employing a late-stage sp^2 C−H oxidation. B) 2nd Gen route employing a late-stage C−H insertion.

as well as diastereo- and enantioselective, method for the preparation of highly substituted benzodihydrofurans.[12−15] At the outset of our alopecurone C campaign, we envisioned a route in which the benzodihydrofuran core would be assembled early in the synthesis with the flavanone ring being added later[16−18] (Figure 2A). This strategy would enable complete modularity and the ability to modify nearly every position of the natural product based on the choice of starting materials. Although the C−H insertion reaction almost always produces cis-configured products, benzodihydrofurans derived from electron-rich benzylic group are known to epimerize to the more thermodynamically favorable trans diastereomers in the presence of Lewis acids, presumably by ring opening to the *para*-quinone methide oxocarbenium ion. This reaction was demonstrated in the isolation of two related natural products[19] and exploited by our group in the first enantioselective synthesis of an oligostilbene natural product.[12]

Due to initial unsuccessful attempts to prepare hydrazones from diortho substituted benzophenones (SI, Figure S1.1), a substrate lacking the second *ortho* alkoxy group was employed (Scheme 1). Given the many advances in the directed functionalization of aromatic C−H bonds with *ortho* carbonyl groups, it was assumed this group could be installed toward the end of the synthesis. The requisite benzophenone precursor **18** was assembled by Friedel−Crafts acylation, regioselective demethylation, and alkylation. As expected, hydrazone formation was straightforward, and the subsequent asymmetric C−H insertion could be executed on decagram scale, producing benzodihydrofuran **10** with excellent stereoselectivity and in high yield employing only 0.1 mol % of dirhodium catalyst. Conversion of the aryl bromide **10** proved difficult through a variety of different cross coupling reactions, necessitating conversion to the iodide under Buchwald's conditions. The resultant iodide was employed without further purification in a Heck reaction to install an acetyl group, which was then used in a second regioselective demethylation with

Scheme 1. Assembly of Advanced Benzodihydrofuran Intermediate 8

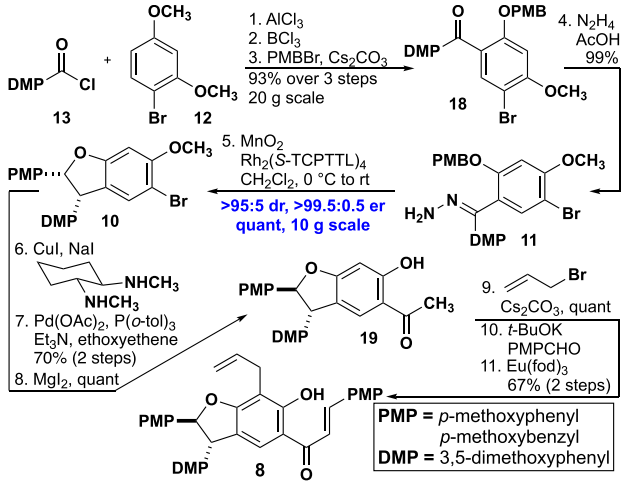

concomitant epimerization of the benzodihydrofuran to the required trans configuration. Alkylation of the phenol with allyl bromide followed by Claisen rearrangement furnished the requisite hydroxychalcone **8**.

Two challenges remained for the synthesis of alopecurone C. First, the flavanone ring needed to be installed with the action of a chiral catalyst. The resultant hydroxychalcone **8** was subjected to a range of different catalysts, none of which produced significant quantities of the flavanone. The electron rich nature of the phenol paired with the added *ortho* substituent resulted in a substrate unsuitable for the catalysts reported to date. We elected to use an unselective cyclization with KF to assess the overall viability of our synthetic route (Scheme 2). After cyclization to produce a 1:1 mixture of diastereomers, the allyl group was converted to a prenyl group using alkene metathesis (**20**).

https://doi.org/10.1021/acs.orglett.4c03863
Org. Lett. 2024, 26, 11129−11133

Scheme 2. Attempted C-5 Functionalization

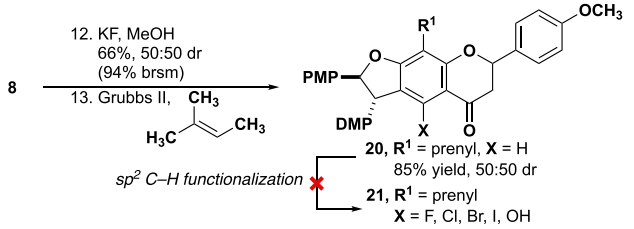

Having assembled the complete tricyclic core of alopecurone C, the second challenge of installing the final alkoxy group by C−H functionalization remained. A series of different catalytic and stoichiometric strategies were employed, none of which produced the desired oxidized flavanone core **21** (Scheme 2). Although this C−H functionalization was addressed through direct *ortho*-lithiation from **10** (SI, Figure S1.2), the required number of steps paired with the unsuccessful stereoselective flavanone installation prompted exploration of a wholly different route.

Recognizing that the entire first-generation route was predicated on the inability to prepare di-*ortho* substituted hydrazones prompted a re-examination of model substrate (Scheme 3). Extensive screening of conditions and additives

Scheme 3. Optimized Hydrazone Formation and C−H Insertion for Di-*ortho*-Substituted Model Ketone 22

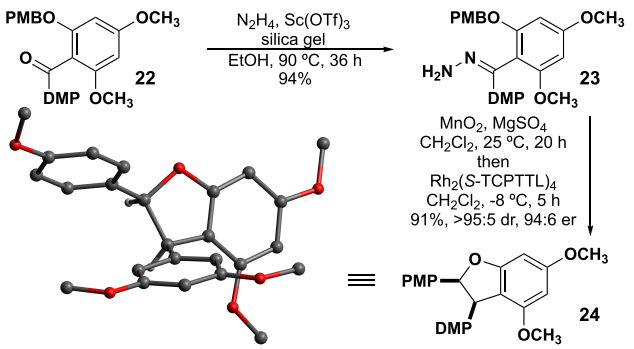

(SI, Table S1.1) revealed that the addition of silica gel and $Sc(OTf)_3$ led to a high yield of hydrazone **23**. Oxidation of this intermediate to the corresponding diazo and subsequent treatment with a chiral rhodium catalyst produced highly substituted benzodihydrofuran **24** in high yield and with high diastereo- and enantioselectivity (SI, Table S1.2). Although the expected cis diastereomer was formed as the major product, the absolute configuration of the product was opposite to **10**, which we attribute to a change in the selectivity-determining step that is also operative with a late-stage intermediate (Scheme 5, *vide infra*).

Armed with this new hydrazone formation and wary of the challenges identified in our first route, we designed a second-generation strategy (Figure 2B). Although the route would be less modular overall, we elected to start with naringenin (**2**) to avoid flavanone synthesis. This route would require protection of the ketone for which we elected to use reduction to the alkane and eventual reoxidation. This tactic was chosen based on the straightforward application of benzylic oxidation to similar targets and the possibility of flavanone epimerization via elimination to the chalcone and recyclization that might occur during ketal formation. Although the requisite starting material, (2*S*)-naringenin **2** (CAS: 480−41−1), is offered by over 50 vendors, the enantiomeric ratio is rarely specified. Despite vendor claims of enantiopurity, we found that (2*S*)-naringenin purchased with a specific claim to be the single enantiomer was actually racemic (SI, Section 6). Despite the difficulty of sourcing the requisite enantiomerically pure flavanone starting material, we elected to test our new route with the racemate.

The required precursor **16** for our second-generation route was accessed through an efficient route from racemic naringenin (Scheme 4). Naringenin could be triply benzoy-

Scheme 4. Synthesis of Hydrazone Intermediate 16 from the Racemic Naringenin (2)

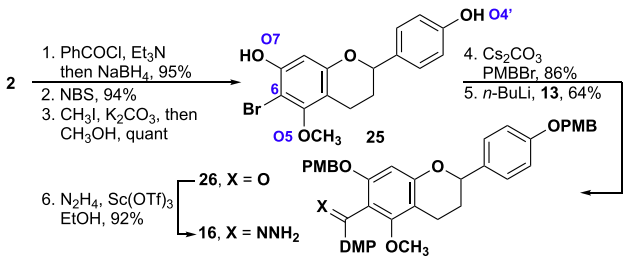

lated, regioselectively deprotected at O5, and concomitantly reduced to the chroman in a single operation with $NaBH_4$. The resultant chroman was then brominated with >95% regioselectivity at C6 with NBS in 94% yield. Finally, methylation with CH_3I and K_2CO_3 followed by saponification with the addition of CH_3OH provided bisphenol **25**, which was then alkylated with PMBBr. The PMB group at O4′ would serve as a protecting group whereas the other PMB group at O7 would provide the C−H insertion site for construction of the benzodihydrofuran. Lithium-halogen exchange with *n*-BuLi and acylation with **13** resulted in benzophenone **26**. Using our new conditions for hydrazone formation (SI, Table S1.3), treatment of **26** with hydrazine and $Sc(OTf)_3$ produced hydrazone **16** in 92% yield.

Hydrazone **16** was carried into our one-pot oxidation and C−H insertion sequence,[12] providing benzodihydrofuran **27** with variable stereoselectivity and yield (Table 1). The absolute and relative stereochemistry were confirmed by X-ray crystallography and computational NMR, respectively (SI, Sections 4/5).[20] Notably, the enantiomeric ratios were 76.2:23.8 (7*S*) and 23.3:76.7 (7*R*) when using the achiral catalyst $Rh_2(TFPTCC)_4$, suggesting substrate control exerted by the remote C7 chiral center (Table 1, entry 1). Chiral catalysts can be employed to override the inherent substrate control. While **28** (entry 2) and many others (SI, Table S1.4) exhibit a mix of catalyst and substrate control, Rh_2(*S*-TFPTTL)$_4$ demonstrated nearly complete catalyst control (entry 3). This result demonstrates that perfect diastereoselectivity would be achieved when a single enantiomer of hydrazone starting material is employed. The high degree of catalyst control in the C−H insertion observed with hydrazone **16** suggests that benzodihydrofuran **27** has the same 2*S*,3*R* configuration observed for **24** (Scheme 3, *vide supra*).

The difference in C−H insertion selectivity for the two routes can be explained by conformational analysis of the rhodium carbene intermediates. Given the small steric demand of the diazo substituent, **11a** and **16a** can readily interconvert between two major conformers (**11a**/**16a**, **11a′**/**16a′**; Scheme

https://doi.org/10.1021/acs.orglett.4c03863
Org. Lett. 2024, 26, 11129−11133

Table 1. Selected Optimization of Insertion Reaction from Hindered Hydrazone 16[b]

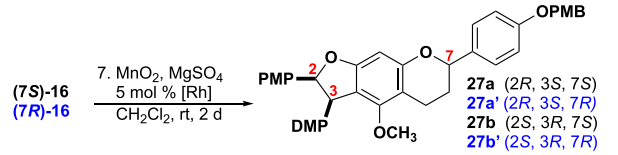

entry[a]	catalyst	dr	er (7S) 27a : 27b	er (7R) 27a' : 27b'	yield
1	Rh_2(TFPTCC)$_4$	75 : 25	38.0 : 11.7	11.9 : 38.5	86%
2	**28**	67 : 33	30.6 : 20.0	12.8 : 36.7	84%
3	Rh_2(*S*-TFPTTL)$_4$	50 : 50	1.4 : 49.6	0.7 : 48.3	91%

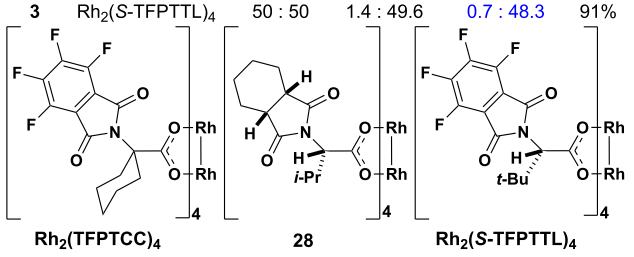

[a]Only cis-2,3-**27** were observed. [b]See Supporting Information for completed catalyst screen.

5, SI, Figure S1.3). In the case of hydrazone **11** (X = H), the mechanism and selectivity-determining step leading to the

Scheme 5. Hypothesis of Different Selectivities of C−H Insertion in Both Routes

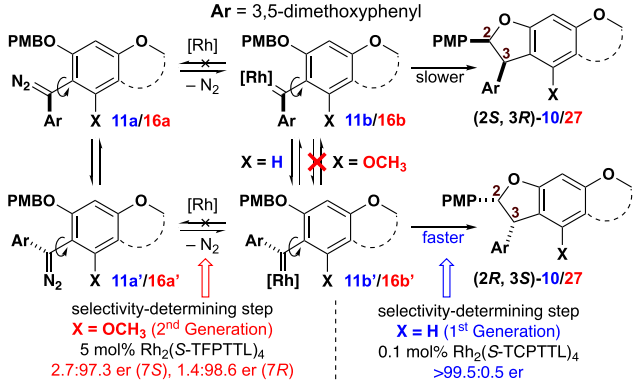

2*R*,3*S* product are consistent with our previous results.[14,15] On the other hand, when X is methoxy, as is the case with the carbene derived from **16**, rotation is probably restricted.[21] As a result, the two conformers of carbene (**16b** and **16b′**) can form at different rates depending on the chiral catalyst employed. After carbene formation, the conformationally restricted carbene undergoes stereoselective hydride transfer and C−C bond formation leading to the major diastereomer. The observation of 2*S*,3*R*-**27** as the major product of C−H insertion is consistent with Rh_2(*S*-TFPTTL)$_4$ preferentially forming carbene from **16a** as opposed to **16a′**.

The complete carbon framework of alopecurone C was achieved by a short synthetic sequence (Scheme 6). Regioselective iodination of **27** and subsequent prenylation by a Suzuki cross-coupling added the final substituent, yielding advanced intermediate **15**. Conversion of **15** to alopecurone C hinged on reinstallation of the flavanone by benzylic oxidation. Unfortunately, various conditions known to achieve this transformation failed to produce the desired ketone (SI, Table S1.5). Although we had hoped to find conditions that would evade this competing oxidation, successful formation of the flavanone was not observed.

Scheme 6. Attempts at Final Benzylic Oxidation

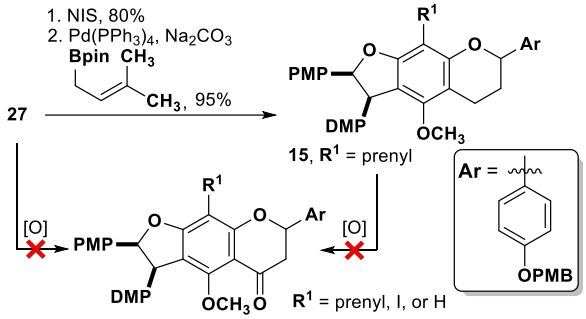

Conclusion

The complete tricyclic core of alopecurone C has been assembled in two stereoselective and high-yielding routes. The first route employed a strategy of maximum modularity that could ultimately lead to the target with the advent of new directed C−H oxidation methods. This route also features the largest scale asymmetric C−H insertion reaction of a donor/donor carbene yet reported, which was accomplished with only 0.1 mol % catalyst. While the second strategy is less modular, it is significantly shorter and is enabled by a new hydrazone-forming reaction that will prove useful in subsequent targets.[5,6,8] The C−H insertion reactions with these di-*ortho*-substituted rhodium carbenes exhibit unique stereocontrol that emanates from selective carbene formation from interconverting conformers. Both strategies highlight the utility of stereoselective C−H insertion of donor/donor carbenes for the assembly of complex benzodihydrofurans. This work represents the first assembly of the carbon frameworks in the flavonostilbene class of natural products and provides access to deoxy analogs that could prove useful for SAR studies.[22] Future work will explore tactics to avoid late-stage manipulations of the flavanone core that will enable the synthesis of alopecurone C and provide a general strategy for related secondary metabolites.

■ ASSOCIATED CONTENT

Data Availability Statement

The data underlying this study are available in the published article and its Supporting Information

Supporting Information

The Supporting Information is available free of charge at https://pubs.acs.org/doi/10.1021/acs.orglett.4c03863.

Experimental procedures, X-ray crystallography data, computational NMR, chiral HPLC spectra, and NMR spectra (PDF)

Accession Codes

Deposition Numbers 2362685, 2390126, and 2390772 contain the supplementary crystallographic data for this paper. These data can be obtained free of charge via the joint Cambridge Crystallographic Data Centre (CCDC) and Fachinformationszentrum Karlsruhe Access Structures service.

https://doi.org/10.1021/acs.orglett.4c03863
Org. Lett. 2024, 26, 11129−11133

AUTHOR INFORMATION

Corresponding Author

Jared T. Shaw − *Department of Chemistry, University of California, Davis, Davis, California 95616, United States;* orcid.org/0000-0001-5190-493X; Email: jtshaw@ucdavis.edu

Authors

Yuan-Shin Shiue − *Department of Chemistry, University of California, Davis, Davis, California 95616, United States*

Matthew W. Dyer − *Department of Chemistry, University of California, Davis, Davis, California 95616, United States*

Noah P. Burlow − *Department of Chemistry, University of California, Davis, Davis, California 95616, United States*

Nutthakarn Soisaeng − *Department of Chemistry, University of California, Davis, Davis, California 95616, United States*

Kellan N. Lamb − *Department of Chemistry, University of California, Davis, Davis, California 95616, United States*

Cristian Soldi − *Department of Chemistry, University of California, Davis, Davis, California 95616, United States*

James C. Fettinger − *Department of Chemistry, University of California, Davis, Davis, California 95616, United States;* orcid.org/0000-0002-6428-4909

Dean J. Tantillo − *Department of Chemistry, University of California, Davis, Davis, California 95616, United States;* orcid.org/0000-0002-2992-8844

Complete contact information is available at: https://pubs.acs.org/10.1021/acs.orglett.4c03863

Notes

The authors declare no competing financial interest.

ACKNOWLEDGMENTS

This work was supported by grants from the National Institutes of Health (R01/GM124234; R35/GM149209) as well as the NSF ACCESS program. This content is exclusively the responsibility of the authors and does not necessarily represent the official views of the National Institutes of Health. We thank the Franz lab (UC Davis) for the use of their chiral HPLC. We thank the National Science Foundation (Grant CHE-1531193) for the Dual Source X-ray diffractometer, and ACCESS program for the computational NMR.

REFERENCES

(1) Baur, J. A.; Sinclair, D. A. Therapeutic Potential of Resveratrol: The in Vivo Evidence. *Nat. Rev. Drug Discovery* **2006**, *5* (6), 493−506.

(2) K. Sahu, N.; S. Balbhadra, S.; Choudhary, J.; V. Kohli, D. Exploring Pharmacological Significance of Chalcone Scaffold: A Review. *Curr. Med. Chem.* **2012**, *19* (2), 209−225.

(3) Keylor, M. H.; Matsuura, B. S.; Stephenson, C. R. J. Chemistry and Biology of Resveratrol-Derived Natural Products. *Chem. Rev.* **2015**, *115* (17), 8976−9027.

(4) Boozari, M.; Soltani, S.; Iranshahi, M. Biologically Active Prenylated Flavonoids from the Genus Sophora and Their Structure−Activity Relationship—A Review. *Phytother. Res.* **2019**, *33* (3), 546−560.

(5) Wan, C. X.; Luo, J. G.; Ren, X. P.; Kong, L. Y. Interconverting Flavonostilbenes with Antibacterial Activity from Sophora Alopecuroides. *Phytochemistry* **2015**, *116* (1), 290−297.

(6) Sato, M.; Tsuchiya, H.; Miyazaki, T.; Ohyama, M.; Tanaka, T.; Iinuma, M. Antibacterial Activity of Flavanostilbenes against Methicillin-resistant Staphylococcus Aureus. *Lett. Appl. Microbiol.* **1995**, *21* (4), 219−222.

(7) Wang, Y.; Zhou, T.; Li, D.; Zhang, X.; Yu, W.; Cai, J.; Wang, G.; Guo, Q.; Yang, X.; Cao, F. The Genetic Diversity and Population Structure of Sophora Alopecuroides (Faboideae) as Determined by Microsatellite Markers Developed from Transcriptome. *PLoS One* **2019**, *14* (12), No. e0226100.

(8) Kwon, J.; Basnet, S.; Lee, J. W.; Seo, E. K.; Tsevegsuren, N.; Hwang, B. Y.; Lee, D. Chemical Constituents Isolated from the Mongolian Medicinal Plant Sophora Alopecuroides L. and Their Inhibitory Effects on LPS-Induced Nitric Oxide Production in RAW 264.7 Macrophages. *Bioorg. Med. Chem. Lett.* **2015**, *25* (16), 3314−3318.

(9) Bergstrom, B. D.; Nickerson, L. A.; Shaw, J. T.; Souza, L. W. Transition Metal Catalyzed Insertion Reactions with Donor/Donor Carbenes. *Angew. Chem., Int. Ed.* **2021**, *60* (13), 6864−6878.

(10) Zhu, D.; Chen, L.; Fan, H.; Yao, Q.; Zhu, S. Recent Progress on Donor and Donor−Donor Carbenes. *Chem. Soc. Rev.* **2020**, *49* (3), 908−950.

(11) He, Y.; Huang, Z.; Wu, K.; Ma, J.; Zhou, Y.-G.; Yu, Z. Recent Advances in Transition-Metal-Catalyzed Carbene Insertion to C−H Bonds. *Chem. Soc. Rev.* **2022**, *51* (7), 2759−2852.

(12) Soldi, C.; Lamb, K. N.; Squitieri, R. A.; González-López, M.; Di Maso, M. J.; Shaw, J. T. Enantioselective Intramolecular C−H Insertion Reactions of Donor−Donor Metal Carbenoids. *J. Am. Chem. Soc.* **2014**, *136* (43), 15142−15145.

(13) Souza, L. W.; Miller, B. R.; Cammarota, R. C.; Lo, A.; Lopez, I.; Shiue, Y.-S.; Bergstrom, B. D.; Dishman, S. N.; Fettinger, J. C.; Sigman, M. S.; Shaw, J. T. Deconvoluting Nonlinear Catalyst−Substrate Effects in the Intramolecular Dirhodium-Catalyzed C−H Insertion of Donor/Donor Carbenes Using Data Science Tools. *ACS Catal.* **2024**, *14* (1), 104−115.

(14) Dishman, S. N.; Laconsay, C. J.; Fettinger, J. C.; Tantillo, D. J.; Shaw, J. T. Divergent Stereochemical Outcomes in the Insertion of Donor/Donor Carbenes into the C−H Bonds of Stereogenic Centers. *Chem. Sci.* **2022**, *13* (4), 1030−1036.

(15) Lamb, K. N.; Squitieri, R. A.; Chintala, S. R.; Kwong, A. J.; Balmond, E. I.; Soldi, C.; Dmitrenko, O.; Castiñeira Reis, M.; Chung, R.; Addison, J. B.; Fettinger, J. C.; Hein, J. E.; Tantillo, D. J.; Fox, J. M.; Shaw, J. T. Synthesis of Benzodihydrofurans by Asymmetric C−H Insertion Reactions of Donor/Donor Rhodium Carbenes. *Chem. Eur. J.* **2017**, *23* (49), 11843−11855.

(16) Zhang, Y.-L.; Wang, Y.-Q. Enantioselective Biomimetic Cyclization of 2′-Hydroxychalcones to Flavanones. *Tetrahedron Lett.* **2014**, *55* (21), 3255−3258.

(17) Maruyama, K.; Tamanaka, K.; Nishinaga, A.; Inada, A.; Nakanishi, T. Conversion of 2′-Hydroxychalcones to Flavanones Catalyzed by Cobalt Schiff Base Complex. *Tetrahedron Lett.* **1989**, *30* (31), 4145−4148.

(18) Hintermann, L.; Dittmer, C. Asymmetric Ion-Pairing Catalysis of the Reversible Cyclization of 2′-Hydroxychalcone to Flavanone: Asymmetric Catalysis of an Equilibrating Reaction. *Eur. J. Org. Chem.* **2012**, *2012* (28), 5573−5584.

(19) Kurihara, H.; Kawabata, J.; Ichikawa, S.; Mizutani, J. (−)-ε-Viniferin and Related Oligostilbenes from Carex Pumita Thunb. (Gyperaceae). *Agric. Biol. Chem.* **1990**, *54* (4), 1097−1099.

(20) Franco, B. A.; Luciano, E. R.; Sarotti, A. M.; Zanardi, M. M. DP4+App: Finding the Best Balance between Computational Cost and Predictive Capacity in the Structure Elucidation Process by DP4+. Factors Analysis and Automation. *J. Nat. Prod.* **2023**, *86* (10), 2360−2367.

(21) Dong, K.; Fan, X.; Pei, C.; Zheng, Y.; Chang, S.; Cai, J.; Qiu, L.; Yu, Z.-X.; Xu, X. Transient-Axial-Chirality Controlled Asymmetric Rhodium-Carbene C(Sp2)-H Functionalization for the Synthesis of Chiral Fluorenes. *Nat. Commun.* **2020**, *11* (1), 2363.

(22) For a preliminary preprint draft of this study, see: Shiue, Y.-S.; et al. Assembly of the Tricyclic Core of Alopecurone C by Asymmetric Donor/Donor Carbene C−H Insertion. *ChemRxiv.* 2024. DOI: 10.26434/chemrxiv-2024-r19z4.